

UNIVERSIDADE FEDERAL DO RIO GRANDE DO SUL  
ESCOLA DE ENGENHARIA - CURSO DE ENGENHARIA MECÂNICA  
TRABALHO DE CONCLUSÃO DE CURSO

STUDY OF CHIP FORMATION MECHANISM IN CFRP TURNING

por

Rodrigo Felipe Klein

Monografia apresentada ao Departamento de Engenharia Mecânica da Escola de Engenharia da Universidade Federal do Rio Grande do Sul, como parte dos requisitos para obtenção do diploma de Engenheiro Mecânico.

Porto Alegre, maio de 2021.

## DADOS INTERNACIONAIS DE CATALOGAÇÃO

Klein, Rodrigo Felipe  
Study of chip formation mechanism in CFRP turning /  
Rodrigo Felipe Klein. -- 2021.  
14 f.  
Orientador: Heraldo José de Amorim.

Trabalho de conclusão de curso (Graduação) --  
Universidade Federal do Rio Grande do Sul, Escola de  
Engenharia, Curso de Engenharia Mecânica, Porto  
Alegre, BR-RS, 2021.

1. CFRP. 2. Turning. 3. Chip formation mechanism.  
4. Tool wear. I. Amorim, Heraldo José de, orient. II.  
Título.

Rodrigo Felipe Klein

STUDY OF CHIP FORMATION MECHANISM IN CFRP TURNING

ESTA MONOGRAFIA FOI JULGADA ADEQUADA COMO PARTE DOS  
REQUISITOS PARA A OBTENÇÃO DO TÍTULO DE  
**ENGENHEIRO MECÂNICO**  
APROVADA EM SUA FORMA FINAL PELA BANCA EXAMINADORA DO  
CURSO DE ENGENHARIA MECÂNICA

Prof. Mário Roland Sobczyk Sobrinho  
Coordenador do Curso de Engenharia Mecânica

Área de Concentração: Processos de Fabricação

Orientador: Prof. Dr. Heraldo José de Amorim

Comissão de Avaliação:

André João de Souza

Heraldo José de Amorim

José Antônio Esmerio Mazzaferro

Porto Alegre, maio de 2021

## AGRADECIMENTOS

Esse espaço será dedicado para todas aquelas pessoas que colaboraram de alguma forma nessa jornada: irmão, avós, sogros, amigos, professores e colegas de estágio e de trabalho, mas principalmente três pessoas em especial. Elas foram fundamentais na minha trajetória acadêmica e principalmente no período da pandemia, onde o apoio foi mais importante ainda.

Meus pais, Solange e Paulo. Nenhuma frase é capaz de representar suficientemente o que fizeram por mim, pois sempre ofereceram forte incentivo desde quando eu comecei a sonhar com a Engenharia em meados de 2013. Tanto o suporte mental, mas principalmente o carinho e a expressão do orgulho em acompanhar meus objetivos foram combustíveis para a minha trajetória. Os principais avanços que eu tive até hoje foram com a motivação, conselhos e ajuda nas tomadas de decisão recebidas deles.

Natalia, minha namorada, participou de boa parte desse período ao meu lado. Foram inúmeras aulas, provas e trabalhos executados com o incentivo, muito amor e orgulho recebidos dela. Sempre com uma mensagem carinhosa ou um abraço, os quais foram fundamentais para que as etapas fossem cumpridas. Além disso, os momentos mais complicados e profundos nesses últimos anos foram vencidos com muito apoio e ajuda dela.

Muito obrigado a todos! Dedico a minha formação a cada um que, em maior ou menor grau, colaborou para esse momento chegar.

UNIVERSIDADE FEDERAL DO RIO GRANDE DO SUL  
 ESCOLA DE ENGENHARIA - CURSO DE ENGENHARIA MECÂNICA  
 TRABALHO DE CONCLUSÃO DE CURSO – 2021

**STUDY OF CHIP FORMATION MECHANISM IN CFRP TURNING**

**Rodrigo Felipe Klein**

rodrigofelipek@gmail.com

***Abstract.** Carbon fiber reinforced polymer (CFRP) is a composite material much less studied than steel and other metals. This material class has excellent properties and allows weight reduction in structural parts; however, the CFRP turning has not the same popularity in the industry of other machining processes as milling and drilling. In this work, a literature survey was conducted to clarify the behavior of CFRP in machining, especially turning. This study evaluated the influence of the composition of the material and the fiber orientation angle, the surface damage during chip formation, and, mainly, parameters as cutting speed, feed rate, depth of cut, and tool geometry and material in the chip formation mechanisms. After discussion, some gaps are identified to be explored using PCD and tools under high cutting parameters conditions. After considering the evaluated studies, an experimental procedure is proposed for future execution, in which the effect of the cutting speed, depth of cut, and tool clearance angle.*

***Keywords:** CFRP, turning, chip formation mechanism, PCD and diamond tool wear.*

**NOMENCLATURE**

Symbols

$\theta$ or $\omega$	Fiber orientation angle	°
$\gamma$	Rake angle	°
$\alpha$	Clearance angle	°
$V_c$	Cutting speed	m/min
$a_p$	Depth of cut	mm
$f_z$	Feed per tooth	mm/tooth
$E$	Elasticity modulus	GPa
$\varepsilon$	Strain	mm/mm
$\sigma$	Stress	MPa
$D$	Stiffness degradation factor	-

Abbreviations

CFRP	Carbon Fiber Reinforced Polymer
GFRP	Glass Fiber Reinforced Polymer
PCD	Polycrystalline Diamond
FEM	Finite Element Model

**INTRODUCTION**

In the last two years, a study named “influence of compressed air cooling on the roughness generated in CFRP end milling” was developed by several fellow students in the Machining

Automation Laboratory at UFRGS. The idea of studying carbon fiber reinforced polymer (CFRP) machining was a challenge since the behavior of this material under machining is much less documented than steel and other metals. The focus was researching how the use of lubricooling methods could influence the machining of this material. After a literature review, an experimental approach was designed, leading to a published paper. This first study was a motivation to keep researching in this field.

The industrial use of CFRP materials has presented considerable growth in the last decades. The main reasons are the properties of these materials: high tensile strength and stiffness, high fatigue resistance, high chemical resistance, and low material density compared to steel and other metals. The excellent resistance to mass ratio makes CFRP a great solution to reduce weight in structures. Furthermore, the production has grown since its application has expanded to the automotive industry and mainly to the aerospace industry (CHEN et al., 2021). Many of the most technological aircraft is composed of over 50% in weight by CFRP.

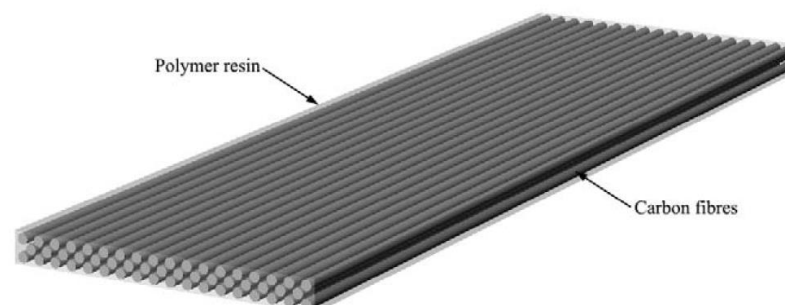
Due to its soft matrix and stiff fiber reinforcement, CFRPs are not homogeneous. Thus, they present anisotropic properties (RAJASEKARAN et al., 2012), which means a chip formation mechanism that is utterly different and more difficult from those observed in the machining of traditional metals (PALANIKUMAR, 2012). Su et al. (2018) reported the material removal mechanism in CFRP machining is not clear yet. Moreover, high abrasive tool wear occurs due to the high abrasive fibers (CEPERO-MEJIAS et al., 2019) and the low thermal conductivity of this composite material, since most of the heat generated during the cutting process is transferred to the tool material, instead of being shared with the work material.

According to Chang (2006), unconventional processes cannot get the shapes obtained by traditional turning, milling, and drilling. Therefore, the traditional material removal processes are the most suitable for machining this material. The current manuscript focus on understanding how the cutting parameters affect the CFRP turning process. After careful literature review, an experimental procedure is proposed to investigate some of the gaps identified in the literature review.

## 2. LITERATURE REVIEW AND STATE-OF-THE-ART

CFRP is composed of carbon fiber embedded in a polymer resin, in which the carbon fiber supports the main load and the second functions as the matrix to hold the fibers (LIU et al. 2015). Fig. 1 illustrates the elements of CFRP material.

Figure 1 – Composite material structure.



Adapted from Liu et al. (2015)

CFRP composites offer greater stiffness and strength than other composite materials. Continuous fibers in an epoxy matrix give the highest performance because the fibers support the mechanical loading, and the matrix material transmits loads to the fibers and provides

ductility and toughness. The matrix material also protects the fibers from any damage. However, on the other hand, it limits the material operation temperature (ASHBY, 2018; LIU et al. 2015). Table 1 presents some characteristics of this material.

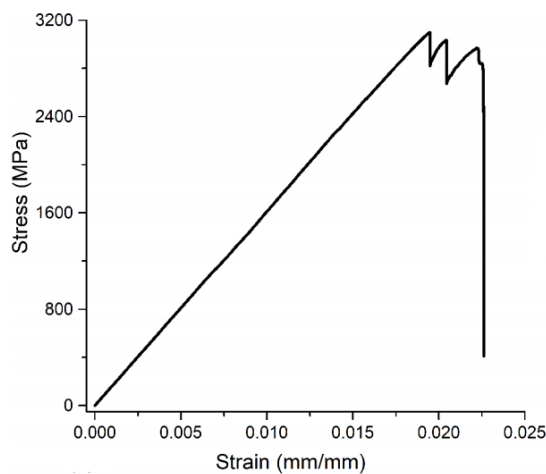
Table 1 – CFRP properties

Property	Range
Density (kg/m <sup>3</sup> )	1,500-1,600
Yield strength (MPa)	550-1,050
Tensile strength (MPa)	550-1,050
Elongation (%)	0.32-0.35
Hardness (HV)	10.8-21.5
Max. temp service (°C)	140-220
Thermal conductivity (W/m.K)	1.28-2.6

Source: Adapted from Ashby (2015)

Hernandez et al. (2017) reported that the material failed without any plastic deformation in the CFRP tensile test, which means the material follows a linear elastic region of deformation until a short unstable zone before rupturing (as shown in Fig. 2). Furthermore, it reported that crack propagation starts in manufacturing defects.

Figure 2 – Composite material composition.



Source: Hernandez et al. (2017)

According to Henerichs et al. (2014), CFRP has been widely used in civil aircraft structures due to its benefits as the low weight, high strength, and corrosion resistance. Boeing 787 and Airbus A350 use around 50 wt. % of this composite material. Moreover, the automotive industry is going to reach a CFRP-production stage.

CFRP materials are used in different forms: plates, tubes, beams, shafts, and specific shapes (wheel, steering wheel, suspension, seat, and others). The present study focuses on revolution forms (tubes and shafts) processed by turning. These forms have an extensive application and are supposed to support loadings like torsion (generated by a torque), flexion (generated by a bending moment), shearing forces and traction.

## 2.1 CFRP machining

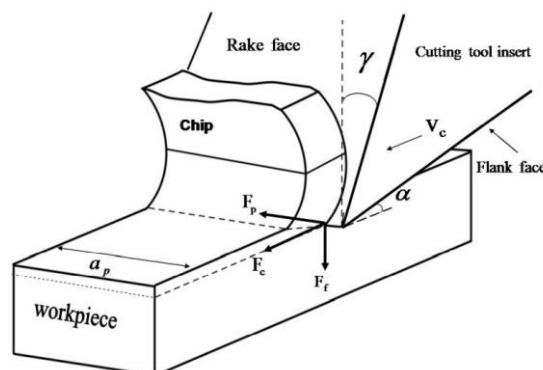
CFRP machining has attracted attention from both academic and industrial research. Several relevant researchers have studied the effects of the fiber orientation, machining parameters, tool geometries and materials nature through the experiment, theory, and simulation methods (SU et al. 2018). However, preliminary research led this study to investigate CFRP turning due to the small number of published papers regarding this combination of material and machining operation. According to Sauer et al. (2020), the machining of rotationally CFRP components is not well documented, with only a few published papers. The authors summarized the importance of turning this material, reporting that lightweight materials have been substituting conventional metals to reduce weight while providing a similar strength, resulting in an increased demand for CFRP shafts. According to Kim et al. (1992), the high demand for CFRP and increased production made this material cheaper. The authors also point that, amongst other properties, this material has a high damping capacity, which helps CFRP structures to dissipate vibrations. Also, due to high stiffness and low mass, the natural frequency of CRFP structures tends to be higher than observed for other materials. Therefore, this material is used in manufacturing high-speed transmission shafts, machine-tool spindles, and robot arms, which means that accurate machining processes are required to provide bearing-mounting and adhesive-joining surfaces.

According to Sauer et al. (2020), this CFRP anisotropy hinders the material machining, resulting in high abrasive tool wear and damages to the work material such as delamination and fiber pull-out. Arola and Ramulu (1996) presented a similar conclusion: according to the authors, abrasive wear of the cutting tool and friction play a dominant role in machining reinforced polymers.

Kim et al (1992) affirmed that the machining of carbon fiber-epoxy composite materials is more complex than machining conventional metals because the wear of sintered-carbide and high-speed steel tools is very critical due to intensive abrasive tool wear caused by the high strength of carbon fibers, thus presenting a challenge for tool lifetime. On the other hand, this difficulty allows precise descriptions of the wear mechanisms for each fiber orientation and tool geometry on orthogonal cutting (HENERICHS et al. 2015), which means a great advantage when studying these effects.

Another important topic when machining this composite is the tool geometry. Some studies proved that carbide tools suffer significant wear, which varies for each tool design. According to Henerichs et al. (2015), the tool wear is strongly orientated toward the tool flank (Fig. 3). Arola and Ramulu (1996) also pointed that abrasive wear occurs predominantly on the tool flank rather than the tool face.

Figure 3 – Tool orientation in CFRP machining.

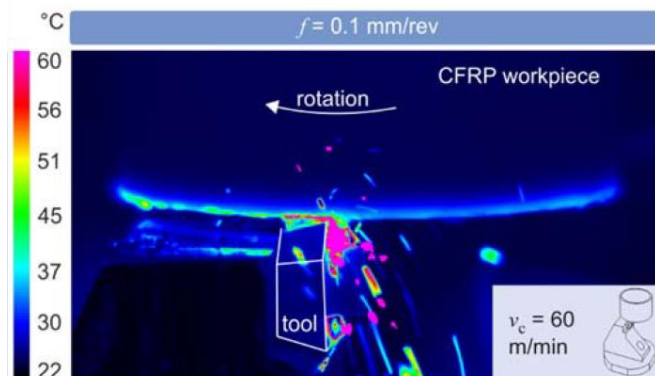


Adapted from Latifzada (2013)



As aforementioned, composites as glass-fiber reinforced polymers (GFRP) and CFRP are heat-insulating materials due to their low thermal conductivity. Thus, most of the heat generated during the cutting process is transferred to the tool, with a minimal part dissipated by the work material. This effect creates a hazardous environment for the cutting tool, allowing wear processes related to high temperatures. Furthermore, there is a significant difference in thermal properties between fiber and matrix material (CHANG, 2006). Still, regarding thermal effects on CFRP turning, Zimmermann et al. (2016) observed important facts. Most mechanical energy is converted into heat during metal cutting due to the plastic deformation of the workpiece material and friction. In CFRP turning, the workpiece is only slightly plastically deformed. However, their study revealed thermal images wherein the workpiece is subjected to a considerable temperature increase during turning. A reason for that can be the heating of the workpiece to be concentrated in a comparatively small material volume due to the low thermal conductivity of the CFRP (Fig. 4).

Figure 4 – Temperature increase in the workpiece during CFRP turning.



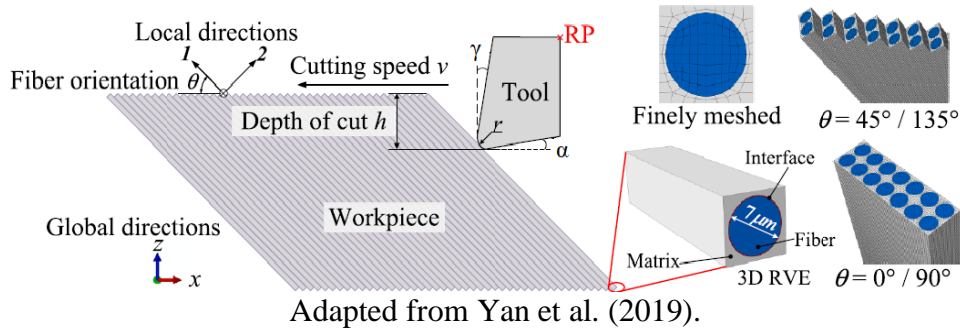
Adapted from Zimmermann et al. (2016).

## 2.2 Matrix and fiber damages

As detailed beforehand, CFRP composites are formed by three elements: epoxy matrix, carbon fibers, and fiber-matrix interface. Below will be described how they have been modeled in several studies, especially with Finite Element Models. Yan et al. (2019) used a discrete-continuum model to analyze the microscopic damage mechanisms involved in the orthogonal cutting of CFRP. Continuum damage mechanics described the progressive softening in the fibers and the matrix. The discrete cohesive zone method was adopted to modeling the traction-separation behavior at the fiber-matrix interface. Figure 5 presents the three CFRP elements and the main parameters involved in machining these materials (fiber orientation, cutting speed, depth of cut, and cutting tool angles). Moreover, two important tool angles can be defined: rake angle ( $\gamma$ ) and clearance angle ( $\alpha$ ). In the figure, the rake angle is positive.

The matrix is an epoxy resin and is usually modeled as an isotropic and elastic-plastic material. Von Mises yield criterion was used for plastic property, and the plastic behavior of the matrix was defined through stress-strain tests. The authors used a ductile failure algorithm to simulate the progressive damage, whose progress was based on linear damage evolution law, as shown in Equation 1 (XU; JIN, 2021).

Figure 5 – CFRP's zones and the main cutting parameters.



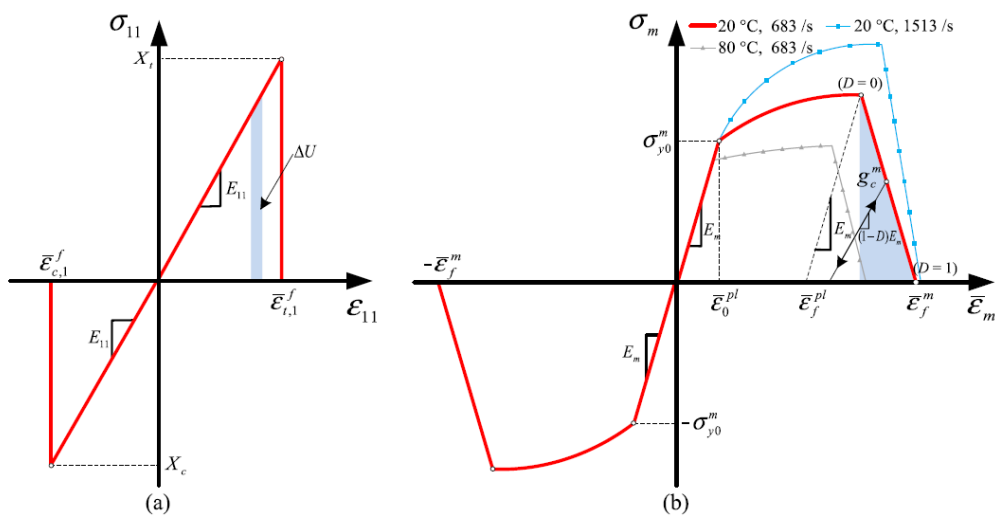
$$\sigma = \left\{ \begin{array}{l} E\varepsilon \\ (1-D)\bar{\sigma} \end{array} \right\} \quad (1)$$

Where  $\sigma$  represents the stress value corresponding to the undamaged status. The stiffness degradation factor  $D$  is zero at the damage initiation point and one after complete failure.

Yan et al. (2019) studied the energy dissipating mechanisms in orthogonal cutting of unidirectional CFRP. Their results showed that the strain rates were typically in the range of  $10^2$  to  $10^6 \text{ s}^{-1}$ . Furthermore, they observed that the temperature variation during orthogonal cutting was higher than  $55^\circ\text{C}$ , which affects the mechanical properties of the matrix. Therefore, the effects of strain rate and temperature on the epoxy matrix were also considered.

In the plastic regime, the elastic modulus of the matrix remains undamaged because it only initiates when the equivalent plastic strain is higher than 5%. So, the  $E_m$  (elastic constant) is equal to 3.35 GPa and linearly degrades until damage saturates at an equivalent plastic strain when the matrix completely loses its load-bearing capacity. At this instant, the fracture energy per unit area the advancing crack is equal to the shaded area in Fig. 6.b (fracture energy density) multiplied by the characteristic length of the element (YAN et al., 2019).

Figure 6 – Stress-strain response: (a) uniaxial tension and compression in the longitudinal direction of the carbon fiber. (b) epoxy matrix under uniaxial tension and compression at several temperatures and strain rates.



(Yan et al., 2019)

Regarding the carbon fibers, they are modeled as transversely isotropic materials and considered pure elastic, without plastic deformation. The maximum stress failure criterion was used, and the authors assumed that the fibers fail when the main tensile/compressive stress exceeds the corresponding strength in each direction. This theory is simple and has been

experimentally proved by several researchers as a great representation of the mechanism of fiber fracture (XU; JIN, 2021). The mathematic model for this theory is presented in Fig. 7.

Figure 7 – A mathematic model for the theory presented.

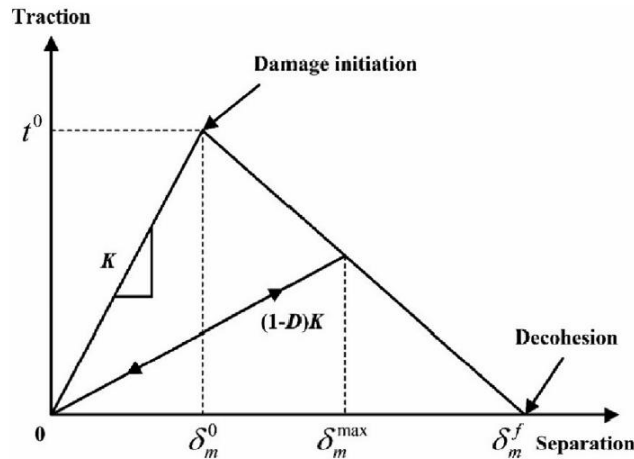
$$\left\{ \begin{array}{l} \text{Tensile failure in longitudinal direction} \quad (\sigma_{11} \geq 0) \quad \left(\frac{\sigma_{11}}{X_T}\right)^2 \geq 1 \\ \text{Compressive failure in longitudinal direction} \quad (\sigma_{11} < 0) \quad \left(\frac{\sigma_{11}}{X_C}\right)^2 \geq 1 \\ \text{Tensile failure in transverse direction} \quad (\sigma_{22} \geq 0 \text{ or } \sigma_{33} \geq 0) \quad \left(\frac{\sigma_{22}}{Y_T}\right)^2 \geq 1, \left(\frac{\sigma_{33}}{Y_T}\right)^2 \geq 1 \\ \text{Compressive failure in transverse direction} \quad (\sigma_{22} < 0 \text{ or } \sigma_{33} < 0) \quad \left(\frac{\sigma_{22}}{Y_C}\right)^2 \geq 1, \left(\frac{\sigma_{33}}{Y_C}\right)^2 \geq 1 \end{array} \right.$$

Adapted from Xu and Jin (2021).

In the model presented in Fig. 7,  $X_T$  (4.9 GPa) and  $X_C$  (3.96 GPa) are tensile and compressive strengths in the longitudinal direction;  $Y_T$  (1.5 GPa) and  $Y_C$  (3.34 GPa) are the tensile and compressive strengths in transverse direction.  $\sigma_{ii}$  is the stress tensor component of the fiber.

The previous description covers the fiber-matrix interface property. There are three classical approaches used in the literature; only the surface-based cohesive behavior used by Xu and Jin (2021) will be described in this section. The linear elastic-separation behavior at the fiber-matrix interface is shown in Fig. 8, where the undamaged response is assumed to be linear-elastic followed by the initiation and evolution of damage. This separated mode is used to simplify the elastic behavior, which indicates that pure normal separation does not affect cohesive stress in the shear directions, and pure shear stress with zero normal separation does not affect normal stress.

Figure 8 – The traction-separation response of the fiber-matrix interface under normal loading.



Adapted from Xu and Jin, 2021.

Ultimately, since most components require a good surface finish, it is important to quote the main surface damage suffered by the material after the machining process. According to Kim et al. (1992), achieving a low surface roughness in the machining of CFRP is not easy, especially if the cutting tool geometry or process parameters are not selected properly. Karatas and Gökkaya (2018) reported that the occurrence of varying failure mechanisms such as these often results in the rejection of numerous components, which causes a crucial demand to

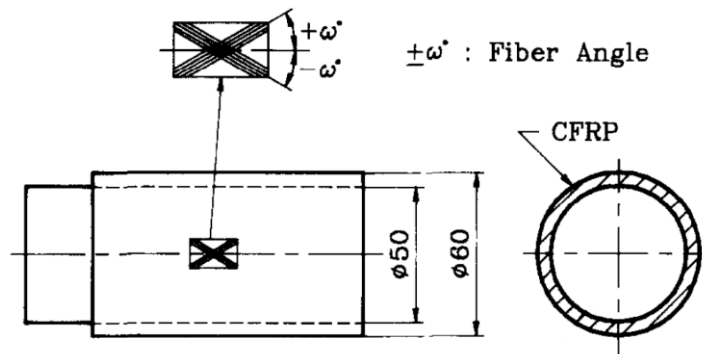
understand the mechanism of machining composites for optimizing the tool design and process planning.

Su et al. (2018) and several other researchers have listed diverse damages that tend to occur during CFRP machining, including delamination, matrix cracking, fiber-matrix debonding, and fiber pull-out that inevitably lead to poor surface quality. Rajasekaran et al. (2012) reached a significant result: increasing cutting speed, the surface roughness decreases, which can be explained by the fact that higher cutting speeds reduce the length of contact between the tool and the chip, reducing the friction in the machining interface. In general, brittle materials deform under rupture; however, the deformation in CFRP composites is a combination of shearing and rupturing. It is also pointed that more fiber had got fractured using higher feed-rates (0.15 mm/rev), increasing the surface roughness.

### 2.3 Chip formation

Fig. 9 presents how the fiber angle  $\omega$  is defined during an orthogonal cutting (in this case, turning). Understanding this is essential because, since this angle influences how the shaft will support an external load, shafts with the same diameter and length are often manufactured with different fiber orientation angles. For instance, if there is an axial load, the fibers must be positioned in the axial length to support tensile stress. However, if there is a torsion load, the fibers must be positioned in the transverse direction. There must be a fiber angle  $\omega$  that will support both axial load and torsion in a mixed case.

Figure 9 – Fiber angle representation on orthogonal cutting

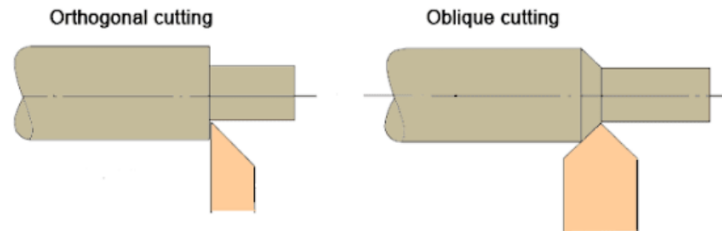


(KIM et al., 1992)

It is essential to highlight that, after the discussion above, the fiber orientation angle  $\omega$  is the main and unique angle to be considered in orthogonal cutting. It is different and more straightforward than other machining processes like milling, where a second angle, named tool oblique, must be considered (Xu and Jin, 2021). These authors reported that, for orthogonal cutting, the cutting area between the tool and the workpiece is small, leading to fiber buckling, followed by a crushing failure with powder (chips with a length typically smaller than 10  $\mu\text{m}$ ).

When analyzing chip formation in a machining process, it is important to understand and define some concepts beforehand. Fig. 10 presents the orthogonal and oblique cutting definitions. In the present study, unidirectional and orthogonal cutting is considered since the tool enters the workpiece perpendicularly and moves in the axial direction.

Figure 10 – Cutting types definition.



Adapted from: Orthogonal cutting and oblique cutting, 2021.

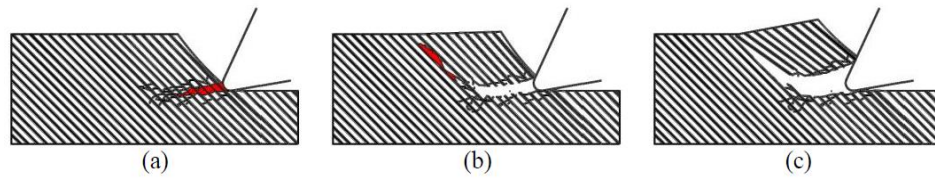
Several authors have published about CFRP behavior during machining, reporting that the chip formation is fundamentally different from the observed for isotropic metals. The insufficient ductility and non-homogeneous properties of the GFRP composites produced discontinuous and fracturing chips during machining operations, generating several material failure modes that seemed to occur randomly along the machined surface (AZMI, 2013). Koplev et al. (1983) observed that the chip thickness corresponds well with the adjusted cutting depth. Furthermore, they noticed the chips had not been subjected to large plastic deformation, generally found in metal chips.

Pwu and Hocheng (1998) used the elementary beam theory and laminate mechanics to construct a chip formation model, describing two stages for perpendicular cutting. At the first contact, the tool cannot cut the fibers and pushes the laminate beam, causing significant deflection. In the second stage, large bending stresses break the fibers, often below the machined surface. However, the fiber failure cannot extend beyond the depth of cut because the matrix material provides resistance to further fiber deformation in the tool direction. The interface between fiber and matrix plays a vital role in stress transmission. As the tool moves in the feed direction, the fractures of the matrix between fibers assist the chip formation. Since the matrix is much weaker than the fiber, chip formation by fiber failure in bending is accompanied with a considerable amount of matrix failure.”

The chip formation and material removal characteristics in orthogonal cutting of CFRP were mainly dependent on fiber orientation (AROLA, RAMULU, 2016; SU et al. 2018; PWU; HOCHENG, 1998). Rao et al. (2007) also observed that the size and shape of the chips depend mainly on the fiber orientation and the depth of cut and, to a lesser extent, of tool geometry. Xu and Jin (2021) reported a strong influence of tool geometry, considering the tool rake angle as a significant parameter. Henerichs et al. (2015) concluded that the increase of the rake angle rake angle combined with a decrease in depth of cut results in larger chips due to the lower material deformation..

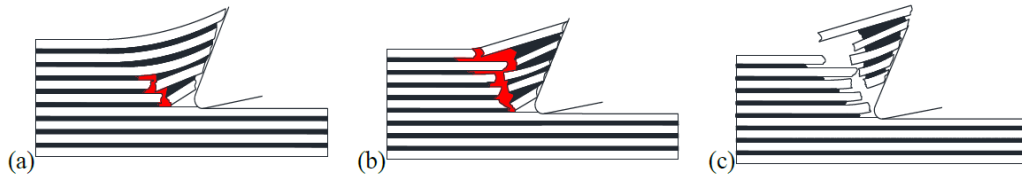
Su et al. (2018) observed that for fiber orientations of 45 ° and 90 °, the chip formation type is cutting (Figure 11), and the material was shattered into powdery particles of fibers and epoxy matrix due to the out-of-plane fracture and crushing-compression of the progressing cutting tool on the workpiece (AZIM, 2013). However, in the case of 0 ° and 135 °, the type of chip formation is debonding-bending (Fig. 12). The depth of cut has little effect on the failure mechanisms in the range of 0.05 mm to 0.15 mm but presents a significant influence on the size of size of chips; since the depth of cut increases, the chip decrease for fiber orientation of 45 °. Regarding rake angle, when positive, it has little effect on the chip formation mechanism but a large effect on the size of chips; as the rake angle increases, the size of chips decreases for fibers oriented at 45 °. However, for fibers oriented at 135 °, a significant influence on the chip formation mechanism is observed. Finally, in the negative rake angle, the failure mechanism in chip formation changes from cutting to crushing.

Figure 11 – Cutting type chip formation.



Adapted from Su et al. (2018)

Figure 12 – Debonding-bending type chip formation.



Adapted from Su et al. (2018)

Zimmermann et al. (2016) realized that both cutting and thrust forces arise by increasing the feed rate. Then, if the feed rate increases, this effect increases the undeformed chip thickness and, thus, the required energy for the material deformation, chip fracture, and chip deflection. Moreover, using higher feed rates, the contact length of the workpiece material with the rake face and the friction work increases during the orthogonal turning. The study by Rajasekaran et al. (2012) also noticed that, as the feed rate increases, the size of chips becomes tiny fine powders, indicating that less strain on the chip produces these fine powders, resulting in a good surface finish.

Azmi (2013) noticed an increase in the cutting speed resulted in smaller chip segmentations, mainly due to increased stress on the chip surface and weak adhesive bonding between the fibers and the epoxy matrix. A similar result was found by Zimmermann et al. (2016), which observed embrittlement of the CFRP after increasing the cutting speed, indicating that it is easier to occur the material fracture at higher cutting speeds, forming smaller chips or dust. The authors observed that large chips and partial fractures were formed at the minimum cutting speed (5 m/min). However, when raising the cutting speed from 60 to 100 m/min the removed material was utterly fractured. Also, they stated that the fracture of the material causes the formation of small chips or dust.

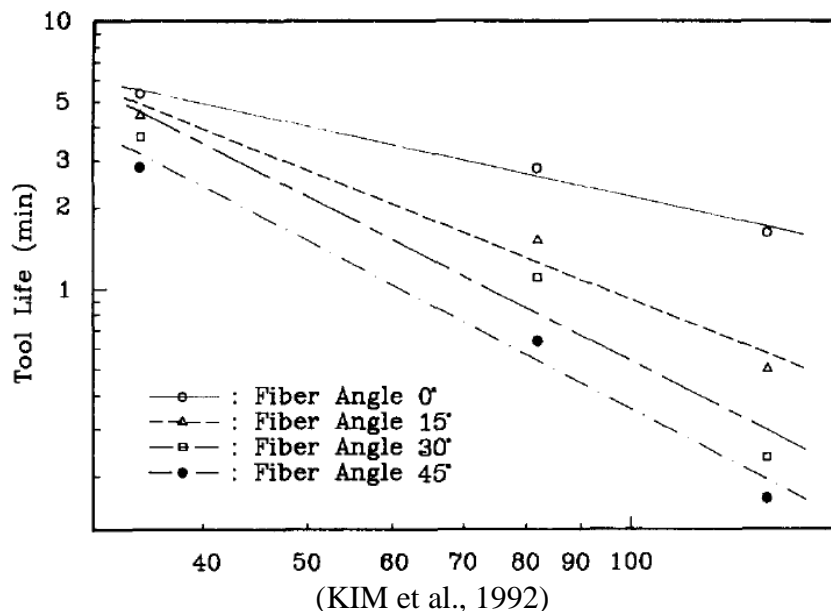
## 2.4 Tool wear

Machining CFRP in a turning operation with a constant fiber orientation (the tubes were manufactured with a single fiber orientation) and using an uncoated carbide insert, Henerichs et al. (2015) observed that the tool suffered strong abrasive wear since it has a low hardness. Thus, cutting materials from PCD or diamond-coated carbide tools were recommended, mainly focusing on the cost-and time-efficient production process. The authors also analyzed the tool flank and postulated a direct relationship between tool wear and feed forces. Based on this, the fiber orientation of  $0^\circ$  and  $150^\circ$  produced the lowest tool wear and forces, being the tool rake angle the main influence factor. The increase of the clearance angle from  $7^\circ$  to  $14^\circ$  resulted in a feed force reduction, while a further increase to  $21^\circ$  did not present significant influence. For fibers oriented on  $30^\circ$  and  $60^\circ$ , the tool wear was higher with smaller clearance angles ( $7^\circ$ ), while greater clearance angles ( $14^\circ$  and  $21^\circ$ ) resulted in lower tool wear. Therefore, this study concluded that: (i) the clearance angle influences more the cutting forces than the rake angle; (ii) low machining force components reduce abrasive wear; (iii) tools with large clearance angles are recommended to achieve the lowest machining forces.

Kim et al. (1992) investigated, experimentally, the machinability of high-strength carbon fiber-epoxy composite materials in turning. The authors could determine the chip formation mechanisms using a high-speed camera and the Taylor tool-life equation. A conclusion was reached that, as usually observed in the machining of metals, tool wear increases with cutting speed and cutting time.

Figure 13 shows that, for low cutting speeds, the tool wear increases with the fiber angle. It occurs due to the cutting angle variation between the fiber and the side rake face of the tool. The cut is orthogonal for  $0^\circ$  fiber angle, but as the fiber angle increases, the fibers are cut obliquely, increasing the cutting force, and inducing more bending effects in the fibers. According to Fig. 13, tool wear is most sensitive to the cutting speed when the fiber angle is  $45^\circ$ . Hence, the fiber angle is the main factor of tool wear in the CFRP machining. Finally, low cutting speeds of 20-40 m/min are recommended when turning with carbide tools because the tool wear rate is very high even at cutting speeds.

Figure 13 – Tool life versus cutting speed for each fiber angle.



Kim et al. (1992) recommended investigating the multi-coated inserts and PCD tools behavior during CFRP machining, focusing on the tool-wear mechanisms. They supposed these materials should be more efficient. It was found in the literature that two decades after, Rajasekaran et al. (2012) machined a CFRP tube with a ceramic tool material, justifying its best performance compared with other tools, such as high hardness and wear resistance.

### 3. METHODOLOGY

After a literature review regarding the main studies developed in the last decades, it is important to identify possibilities to investigate. Several authors pointed some areas to continue the tests or gaps that their studies could not cover for specific reasons. Thus, this chapter will be divided into two analyses: preliminary and experimental. The first one will present a table containing the cutting parameters and variables used in several studies. Thereby, this table will guide the second analysis, where preliminary tests (an experimental matrix) will be proposed varying cutting parameters.

### 3.1 Preliminary analysis based on the literature

The literature review regarded how the various parameters involved in the machining of CFRP affected the results of the variables. Table 2 presents the parameters and values used in the main literature studies and which phenomena were evaluated. This evaluation is fundamental to obtain functional windows for the experiments proposed.

Table 2 – Cutting parameters used by previous CFRP turning papers

Parameters	Henerichs	Sauer	Kim	Rajasekaran	Zimmerman	Dold
$\theta$ (°)	0, 30, 60, 90, 150	15	-	-	45, 135	30, 90, 150
$V_c$ (m/min)	90	100	25 - 30	100, 200, 300	20, 40, 60, 80, 100	200
$f_z$ (mm/rev)	0.3	0.05 to 0.2	0.11	0.05 to 0.15	0.025 to 0.4	0.1
$a_p$ (mm)	-	0.1, 0.4, 0.6	0.2	0.5 to 1.50	2	1
$\gamma$ (°)	0 to 30	5 and 7	6	-	0	0
$\alpha$ (°)	7 and 21	-	-	-	15	7
Tool material	Uncoated Carbide	Uncoated Carbide	Uncoated Carbide	Ceramic	Uncoated Carbide	PCD
Evaluated phenomena	Process forces Surface Tool wear	Process forces Surface	- Surface Tool wear	- Surface -	Chip formation Temperature	Tool wear

The studies presented in Table 2 show that only Zimmermann et al. (2016) explored the chip formation mechanism, while two papers analyzed the tool wear. Surface quality and force components are the most evaluated parameters, and it has also been also observed for drilling and milling. Therefore, the experimental analysis will focus on the chip formation mechanism and the tool wear. The fiber angle orientation, the cutting tool material, and the feed rate will be fixed, but the cutting speed, clearance angle, and depth of cut will be varied.

### 3.2 Experimental analysis

From the literature survey, since most CFRP turning experiments used uncoated carbide tools, there is a gap in PCD or diamond-coated carbide tool wear behavior. One paper used ceramic tools (harder than carbide tools). However, the authors focused on measuring surface roughness in turning, which did not solve an essential gap regarding how diamond-coated carbide tools behave. From the study of Henerichs et al. (2015), it is known that uncoated carbide tools present intensive wear.

Regarding the chip formation mechanism, the cutting speed has been reported as the main cutting parameter influence. In Tab. 2, several authors used values up to 100 m/min for carbide tools, while Rajasekaran et al. (2012) used higher cutting speeds, from 100 up to 300 m/min with a ceramic tool. However, diamond tools are more wear-resistant than ceramic and carbide tools and support higher cutting speeds (up to 600 m/min) according to the manufacturer (J&M Diamond Tool, 2001). Thereby, it is important to analyze how the chips are formed, and the tool wear occurs at higher cutting speeds.



About the feed rate, it has a low impact on the chip formation mechanism. Hence, it also can be fixed at 0.1 mm/rev for the material economy, which is significant since CFRP shafts are not ordinary material. Furthermore, the tool manufacturer J&M Diamond Tool (2001) indicates this as the maximum value.

For the evaluation of the tool wear it is essential to know the fiber orientation angle. According to Fig. 13, tool wear increases with both the cutting speed and the fiber angle. CFRP shafts are usually produced with fiber orientation angles at 45 ° to promote adequate resistance to traction and torsion. Therefore, the experiments shall be conducted with fiber orientation angles near to 45 ° and the highest cutting speed applicable to allow the worst tool wear case (shortest tool life).

According to Su et al. (2018), depth of cut has little effect on the failure mechanisms in a range from 0.05 to 0.15 mm. Meanwhile, the chip sizes decrease as the depth of cut increases in fiber orientation at 45 °. It is interesting to evaluate this phenomenon, especially for high cutting depths (between 0.5 and 1.5 mm), according to Rajasekaran et al (2012).

The last parameter evaluated in more than one level will be the tool clearance angle. According to Henerichs et al. (2015), the clearance strongly influences over the cutting forces than the rake angle. Moreover, the authors concluded that, for 30 ° and 60 ° fiber orientation, the tool wear was higher with smaller clearance angles (7 °), while greater clearance angles (14 ° and 21 °) showed lower wear rates. Based on that, and since a few studies evaluated this parameter, it is recommended to vary this angle and observe its influence on the tool wear.

Table 3 presents the recommended parameters for the experimental evaluation of the influence of the process parameters on the orthogonal turning of CFRP shafts. Two experiments are proposed with different tool materials: uncoated carbide and PCD. Both experiments are factorial and must be executed with three runs.

Table 3 – Recommended variable parameters for the proposed experiments.

Tool material	Parameter	Minimum	Medium	Maximum
Uncoated Carbide	Cutting speed (m/min)	50	100	150
	Depth of cut (mm)	0.5	1.0	1.5
	Clearance angle ( $\alpha$ ) (°)	7°	-	21°
PCD	Cutting speed (m/min)	200	400	600
	Depth of cut (mm)	0.5	1.0	1.5
	Clearance angle ( $\alpha$ ) (°)	7°	-	21°

Appendix A shows an experimental matrix wherein these parameters (Tab. 3) were combined to execute eighteen experimental conditions that must be tested with three runs. These tests could be executed in a manual lathe. However, due to some aggressive cutting conditions, a CNC is recommended to ensure better precision and reliability.

As described before, there are two main phenomena to be analyzed: chip formation mechanism and the amount of tool wear. The former will be observed in slow motion through a high-speed camera. Kim et al. (1992) and Zimmermann et al. (2016) also used resources to assess the chip formation in turning, but with very different cutting conditions. These studies will be a reference to analyze the footage recorded and to discuss the phenomena observed since the material removal mechanism expected is a combination of buckling, bending, and peeling. The expected results are some qualitative analyses regarding the beginning, development, and finishing steps of the chip formation as type (continuous or discontinuous chip), morphology (powder, short rod, long or rolled), exit direction related to the direction of the tool rake face.

The tool wear will be periodically measured throughout the tests using a Dino-Lite AM-413ZT USB digital microscope from the Manufacturing Automation Laboratory (LAUS).

Other related information might be measured during tests using available resources in the lab, such as the force components measured with a Kistler 9129A piezoelectric dynamometer and the surface roughness with a SJ-201P Mitutoyo rugosimeter.

#### **4. CONCLUSION**

Based on the literature review developed and the papers read, this study recommends a factorial design of experiments. The recommended procedure is presented in an experimental matrix (appendix A), where cutting speed, tool clearance angle, and depth of cut will be used in different levels to investigate the chip formation mechanism (type, size, morphology, and exit direction) and the tool wear (material volume lost) for carbide and PCD tools in the turning of 45 ° fiber oriented CFRP shafts. The recommended values are literature-based references and must be adjusted for the cutting tools available.

## REFERENCES

- AROLA, D.; RAMULU, M. Orthogonal cutting of fiber-reinforced composites: a finite element analysis. **International Journal of Mechanical Sciences**, v. 39, p. 597-613, 1997. [https://doi.org/10.1016/S0020-7403\(96\)00061-6](https://doi.org/10.1016/S0020-7403(96)00061-6)
- ASHBY, M. F. Materials and the environment, Chapter 15 – Material Profiles. **Butterworth-Heinemann**, v.2, p. 459-595, 2013.
- AZMI, A. I. Chip formation studies in machining fiber reinforced polymer composites. **International Journal of Materials and Product Technology**, p. 31-46, 2013. <https://www.researchgate.net/publication/264836662>
- CEPERO-MEJIAS, F.; CURIEL-SOSA, J. L.; KERRIGAN, K.; PHADNIS, V. A. Chip formation in machining of unidirectional carbon fiber reinforced polymer laminates: FEM based assessment. **Procedia CIRP**, v. 85, p. 302-307, 2019. <https://doi.org/10.1016/j.procir.2019.09.005>
- CHEN, Y.; YE, L.; FU, K. Progressive failure of CFRP tubes reinforced with composite sandwich panels: Numerical analysis and energy absorption. **Composite structures**, v. 263, p. 113674, 2021. <https://doi.org/10.1016/j.compstruct.2021.113674>
- CHANG, C. S. Turning of glass-fiber reinforced plastics materials with chamfered main cutting-edge carbide tools. **Journal of Materials Processing Technology**. v. 180, p. 117-129, 2006. <https://doi.org/10.1016/j.jmatprotec.2006.05.011>
- DOLD, C.; HENERICHS, M.; BOCHMANN, L.; WEGENER, K. Comparison of ground and laser machined polycrystalline diamond (PCD) tools in cutting carbon fiber reinforced plastics (CFRP) for aircraft structures. **Procedia CIRP**, v. 1, p. 178-183, 2012. <https://doi.org/10.1016/j.procir.2012.04.031>
- HENERICHS, M.; VOSS, R.; KUSTER, F.; WEGENER, K. Machining of carbon fiber reinforced plastics: influence of tool geometry and fiber orientation on the machining forces. **CIRP Journal of Manufacturing Science and Technology**. v. 9, p. 136-145, 2015. <http://dx.doi.org/10.1016/j.cirpj.2014.11.002>
- HERNANDEZ, D. A.; SOUFEN, C. A.; ORLANDI, M. O. Carbon fiber reinforced Polymer and epoxy adhesive tensile teste failure analysis using scanning electron microscopy. **Materials Research**, v. 20, n. 4, 2017. <https://doi.org/10.1590/1980-5373-mr-2017-0229>
- KARATAS, M. A.; GÖKKAYA, H. A review on machinability of carbon fiber reinforced polymer (CFRP) and glass fiber reinforced polymer (GFRP) composite materials. **Defence Technology**, v. 14, p. 318-326, 2018. <https://doi.org/10.1016/j.dt.2018.02.001>
- KOPLEV, A.; LYSTRUP, A.; VORM, T. The cutting process, chips and cutting forces in machining CFRP. **Composites**. v. 14, p. 371-376, 1983. [https://doi.org/10.1016/0010-4361\(83\)90157-X](https://doi.org/10.1016/0010-4361(83)90157-X)
- J&M Diamond Tool, Inc. Composition of PCD and CBN. 2001. Available in: < [J & M Diamond Tool: PCD and CBN Information](#)>. Accessed on Apr 20, 2021.

KIM, K. S.; LEE, D. G.; KWAK, Y. K.; NAMGUNG, S. Machinability of carbon fiber-epoxy composite materials in turning. **Journal of Materials Processing Technology**. v. 32, p. 553-570, 1992. [https://doi.org/10.1016/0924-0136\(92\)90253-O](https://doi.org/10.1016/0924-0136(92)90253-O)

LATIFZADA, M. A. Estimation of flank wear growth on coated inserts. **Uppsala Universitet**, Master program in Physics, p. 4, 2013.

LIU, Y.; ZWINGMANN, B.; SCHLAICH, M. Carbon fiber reinforced polymer for cable structures – A review. **Polymers**, v. 7, p. 2078-2099, 2015. <https://doi.org/10.3390/polym7101501>

Orthogonal cutting and oblique cutting. **Mecholic**. Available in: [Orthogonal Cutting and Oblique Cutting | Mecholic](#). Accessed on Apr, 24, 2021.

PALANIKUMAR, K. Analysing surface quality in machined composites. **Machining technology for composite materials**, pp. 154-182, 2012. <https://doi.org/10.1533/9780857095145.1.154>

PWU, H. Y.; HOCHENG, H. Chip formation model of cutting Fiber-Reinforced Plastics perpendicular to fiber axis. **Journal of Manufacturing Science and Engineering**, v. 120, p. 192-196, 1998. <https://doi.org/10.1115/1.2830100>

RAJASEKARAN, T.; PALANIKUMAR, K.; VINAYAGAM, B. K. Turning CFRP composite with ceramic tool for surface roughness analysis. **Procedia Engineering**. v. 38, p. 2922-2929, 2012. <https://doi.org/10.1016/j.proeng.2012.06.341>

RAO, G. V. G.; MAHAJAN, P.; BHATNAGAR, N. Machining of UD-GFRP composites chip formation mechanism. **Composites Science and Technology**, v. 67, p. 2271-2281, 2007. <https://doi.org/10.1016/j.compscitech.2007.01.025>

SAUER, K.; HERTEL, M.; FICKERT, S.; WITT, M.; PUTZ, M. Cutting parameter study of CFRP machining by turning and turn-milling. **Procedia CIRP**. v. 88, p. 457-461, 2020. <https://doi.org/10.1016/j.procir.2020.05.079>

SU, Y.; UM, S.; WANG, C.; Xu, H.; YANG, H. Chip formation mechanism in machining of carbon fiber reinforced plastic. **Materials Science**, p. 161-171, 2018. <https://doi.org/10.12783/dtcse%2Fcmsms2018%2F25198>

XU, X.; JIN, X. 3-D finite element modeling of sequential oblique cutting of unidirectional carbon fiber reinforced polymer. **Composite structures**, Vol. 256, pp. 113-127, 2021. <https://doi.org/10.1016/j.compstruct.2020.113127>

YAN, X.; REINER, J.; BACCA, M.; ALTINTAS, Y.; VAZIRI, R. A study of energy dissipating mechanisms in orthogonal cutting of UD-CFRP composites. **Composite structures**. v. 220, p. 460-472, 2019. <https://doi.org/10.1016/j.compstruct.2019.03.090>

ZIMMERMANN, M.; HEBERGER, L.; SCHNEIDER, F.; EFFGEN, C.; AURICH, J. C. Investigation of chip formation and workpiece load when machining carbon-fiber-reinforced-polymer (CFRP). **Procedia Manufacturing**, v. 6, p. 124-133, 2016. <https://doi.org/10.1016/j.promfg.2016.11.016>

## APPENDIX A

### Observation:

1. Each test number must be executed three times (three runs)
2. The execution order of the tests must be shuffled before the beginning of each run.
3. Table A.1 presents the experimental matrix for the execution of tests with PCD tools. For the execution of tests with carbide tools, the three levels of cutting speed must be replaced by adequate levels according to Tab. 3.

Table A.1 - Experimental matrix for the tests performed with PCD tools.

Test number	Clearance angle (°)	Cutting speed (m/min)	Depth of cut (mm)
1	7	200	0.5
2	7	200	1.0
3	7	200	1.5
4	7	400	0.5
5	7	400	1.0
6	7	400	1.5
7	7	600	0.5
8	7	600	1.0
9	7	600	1.5
10	21	200	0.5
11	21	200	1.0
12	21	200	1.5
13	21	400	0.5
14	21	400	1.0
15	21	400	1.5
16	21	600	0.5
17	21	600	1.0
18	21	600	1.5